G Protein–Coupled Receptor Kinase 2 Activity Impairs Cardiac Glucose Uptake and Promotes Insulin Resistance After Myocardial Ischemia

Michele Ciccarelli, MD, PhD; J. Kurt Chuprun, PhD; Giuseppe Rengo, MD, PhD; Erhe Gao, MD, PhD; Zhengyu Wei, PhD; Raymond J. Peroutka, BS; Jessica I. Gold, BS; Anna Gumpert, PhD; Mai Chen, MD, PhD; Nicholas J. Otis, BS; Gerald W. Dorn II, MD; Bruno Trimarco, MD; Guido Iaccarino, MD, PhD; Walter J. Koch, PhD

Background—Alterations in cardiac energy metabolism downstream of neurohormonal stimulation play a crucial role in the pathogenesis of heart failure. The chronic adrenergic stimulation that accompanies heart failure is a signaling abnormality that leads to the upregulation of G protein–coupled receptor kinase 2 (GRK2), which is pathological in the myocyte during disease progression in part owing to uncoupling of the β-adrenergic receptor system. In this study, we explored the possibility that enhanced GRK2 expression and activity, as seen during heart failure, can negatively affect cardiac metabolism as part of its pathogenic profile.

Methods and Results—Positron emission tomography studies revealed in transgenic mice that cardiac-specific overexpression of GRK2 negatively affected cardiac metabolism by inhibiting glucose uptake and desensitization of insulin signaling, which increases after ischemic injury and precedes heart failure development. Mechanistically, GRK2 interacts with and directly phosphorylates insulin receptor substrate-1 in cardiomyocytes, causing insulin-dependent negative signaling feedback, including inhibition of membrane translocation of the glucose transporter GLUT4. This identifies insulin receptor substrate-1 as a novel nonreceptor target for GRK2 and represents a new pathological mechanism for this kinase in the failing heart. Importantly, inhibition of GRK2 activity prevents postischemic defects in myocardial insulin signaling and improves cardiac metabolism via normalized glucose uptake, which appears to participate in GRK2-targeted prevention of heart failure.

Conclusions—Our data provide novel insights into how GRK2 is pathological in the injured heart. Moreover, it appears to be a critical mechanistic link within neurohormonal crosstalk governing cardiac contractile signaling/function through β-adrenergic receptors and metabolism through the insulin receptor. **(*Circulation*. 2011;123:1953-1962.)**

Key Words: glucose ■ heart failure ■ myocardial ischemia ■ positron-emission tomography

Despite improvements in the treatment of heart failure (HF), the prognosis of this disease remains poor.[1,2] The reason that HF continues to worsen even in patients receiving optimal therapy is unclear; however, there is increasing evidence that perturbations in cardiac metabolism can contribute to the progression of cardiomyopathy and to a loss of pharmacological effectiveness.[3,4] Therefore, approaches targeting more efficient substrate use and preservation of cardiac metabolism are attractive therapeutic strategies.[5] In the adult heart, the major pathway for ATP production is fatty acid oxidation,[6,7] whereas the relative contribution of glucose increases during stress or injury such as during exercise or ischemia.[5] During HF, there are excessive uptake and myocardial free fatty acid accumulation with reduced glucose use.[8,9] In animal models of HF and in human disease, these metabolic alterations reduce myocardial oxygen efficiency and lead to a depletion of intracellular ATP.[10,11]

Clinical Perspective on p 1962

Insulin receptor signaling is critically involved in increasing glucose uptake in the myocardium, and cardiac insulin resistance contributes to the development of left ventricular (LV) dysfunction by reducing cardiac efficiency through metabolic shift toward fatty acids use.[12] Indeed, a profound

Received September 9, 2010; accepted March 1, 2011.

From the George Zallie and Family Laboratory for Cardiovascular Gene Therapy, Center for Translational Medicine, Thomas Jefferson University, Philadelphia, PA (M. Ciccarelli, J.K.C., G.R., E.G., Z.W., R.J.P., J.I.G., A.G., M. Chen, N.J.P., W.J.K.); Department of Clinical Medicine and Cardiovascular Science, "Federico II" University of Naples, Naples, Italy (M. Ciccarelli, B.T.); Division of Cardiology, Fondazione "Salvatore Maugeri"–IRCCS–Istituto di Telese Terme, Benevento, Italy (G.R.); Center for Pharmacogenomics, Department of Internal Medicine, Washington University School of Medicine, St. Louis, MO (G.W.D.); and University of Salerno, Department of Medicine, Salerno, Italy (G.I.).

The online-only Data Supplement is available with this article at http://circ.ahajournals.org/cgi/content/full/CIRCULATIONAHA.110.988642/DC1.

Correspondence to Walter J. Koch, PhD, FAHA, W.W. Smith Professor of Medicine and Director, Center for Translational Medicine, Thomas Jefferson University, 1025 Walnut St, Room 317, Philadelphia, PA 19107. E-mail walter.koch@jefferson.edu

Circulation **is available at http://circ.ahajournals.org** **DOI: 10.1161/CIRCULATIONAHA.110.988642**

state of insulin resistance has been found in the hearts of *ob/ob* mice, and the ability of these hearts to modulate substrate use in response to insulin and changes in fatty acid supply is altered.[13] Importantly, normalization of cardiac metabolism by overexpressing a human GLUT4 transgene in mice with insulin resistance recovered the altered cardiac function observed in these animals.[14,15] Therefore, these studies indicate that cardiac insulin resistance reduces the metabolic efficiency of the heart, which can lead to contractile dysfunction. Moreover, insulin resistance is a known and recognized phenomenon leading to HF,[16] as seen in positron emission tomographic (PET) studies showing that failing human myocardium has reduced glucose uptake and increased free fatty acid uptake.[17]

Several hypotheses have been proposed to explain the association between altered cardiac metabolism, insulin resistance, and HF. Among these hypotheses, there is a strong correlation with neurohormonal activation,[18,19] which increases plasma free fatty acid levels and inhibits insulin receptor signaling, resulting in a loss of myocyte glucose uptake.[20] An important abnormality in the myocyte induced by neurohormonal activation in HF is the upregulation of G protein–coupled receptor kinase 2 (GRK2), which classically phosphorylates activated G protein–coupled receptors such as the β-adrenergic receptors (βARs) in the heart, leading to attenuated signaling.[21] In human HF, increased GRK2 is associated with lower cardiac function and prognosis.[22,23]

Recent evidence suggests that GRK2 can have non–G protein–coupled receptor effects, including playing an unidentified role in the regulation of insulin signaling in noncardiac cells.[24,25] Moreover, increases in GRK2 activity after βAR stimulation inhibit insulin-dependent glucose extraction.[26] Therefore, we hypothesized that increased levels of GRK2, as seen during HF, directly induce myocardial insulin resistance, and given the importance of cardiac signaling for efficient metabolic substrate use, we have studied the role of GRK2 in regulating cardiac insulin signaling and metabolism in normal and postischemic myocytes and hearts. Our data reveal a role for GRK2 in HF pathogenesis that extends beyond the known negative effects on βAR signaling and cardiac contractility by demonstrating that GRK2 can critically and negatively affect cardiac insulin signaling and metabolism.

Methods

Experimental Procedures

Experimental procedures were performed essentially as described previously.[27,28] An expanded Methods section appears in the online-only Data Supplement.

Statistical Analyses

All experiments were performed at least in triplicate using cell isolates from different rats. The results were expressed as mean±SEM. We used Prism 4 and SPSS 17 to perform statistical analysis with a 2-tailed Student *t* test for in vitro studies and 2-way and repeated measures ANOVA with a Bonferroni posthoc test for the in vivo studies. SPSS was used to evaluate the normal distribution according to the Levene test for normality and to provide different *P* values for unpaired samples, depending on normal distribution. Even when the data are not normally distributed, we still found significant differences between means of different treatments and/or groups. A value of $P<0.05$ was considered statistically significant.

Results

G Protein–Coupled Receptor Kinase 2 Levels Influence In Vivo Cardiac Glucose Uptake

We first examined whether increased GRK2 in cardiomyocytes can alter in vivo glucose uptake in the hearts of mice after insulin treatment. This is important because myocardial GRK2 upregulation occurs immediately after ischemic injury[29] and may trigger further signaling defects. Therefore, we performed micro-PET using 18-fluorodeoxyglucose (18-FDG) in transgenic mice with cardiac-specific GRK2 overexpression (Tg-GRK2[30]) and their nontransgenic littermate controls (NLCs). An insulin injection produces a robust increase in in vivo 18-FDG accumulation in the hearts of NLC mice, which is significantly lower in Tg-GRK2 mice (Figure 1A). Mechanistically, GRK2 enhancement appears to cause a loss of insulin-dependent GLUT4 membrane translocation (Figure 1B).

G Protein–Coupled Receptor Kinase 2 Regulation of Insulin Signaling in Cardiomyocytes

Because of the above provocative in vivo results, we explored molecular mechanisms involving GRK2 and insulin signaling in cultured adult rat ventricular cardiomyocytes (ARVMs). As expected, when ARVMs were exposed to insulin, GLUT4 membrane translocation was induced, as was the activation of the downstream kinase, Akt (Figure 2A through 2C). Unexpectedly, we found that insulin induced the membrane translocation of GRK2 (Figure 2A and 2D). The cause of GRK2 membrane translocation after insulin administration is unclear, but we next evaluated whether increased membrane GRK2 levels could alter downstream insulin receptor signaling. To do this, we prestimulated ARVMs with the βAR agonist isoproterenol to cause G$\beta\gamma$-dependent GRK2 translocation, which was evident in ARVMs (Figure 2A and 2). Interestingly, after isoproterenol pretreatment, insulin failed to induce GLUT4 translocation, and there was significantly less insulin-dependent Akt activation (Figure 2A through 2C).

To further explore how GRK2 levels may alter myocyte insulin signaling, we overexpressed GRK2 in ARVMs using an adenovirus (AD; ADGRK2). We found that increased GRK2 in ARVMs attenuated insulin-stimulated Akt activation and GLUT4 membrane translocation compared with control myocytes infected with AD green fluorescent protein (GFP; Figure 3A and 3B). Reduced GLUT4 translocation is consistent with the above findings in Tg-GRK2 mice showing that enhanced GRK2 can lead to a loss of insulin-dependent in vivo cardiac glucose uptake. Indeed, we found that insulin-dependent [H^3]-deoxyglucose uptake in ARVMs was significantly attenuated by ADGRK2 (Figure 3C).

G Protein–Coupled Receptor Kinase 2 Activity Is Required for Attenuation of Cardiomyocyte Insulin Signaling via Direct Phosphorylation of Insulin Receptor Substrate-1

Mechanistically, GRK2 could exert its inhibitory effect on insulin-dependent GLUT4 translocation and cardiomyocyte glucose uptake and metabolism through different pathways. GLUT4 membrane translocation has been shown to be

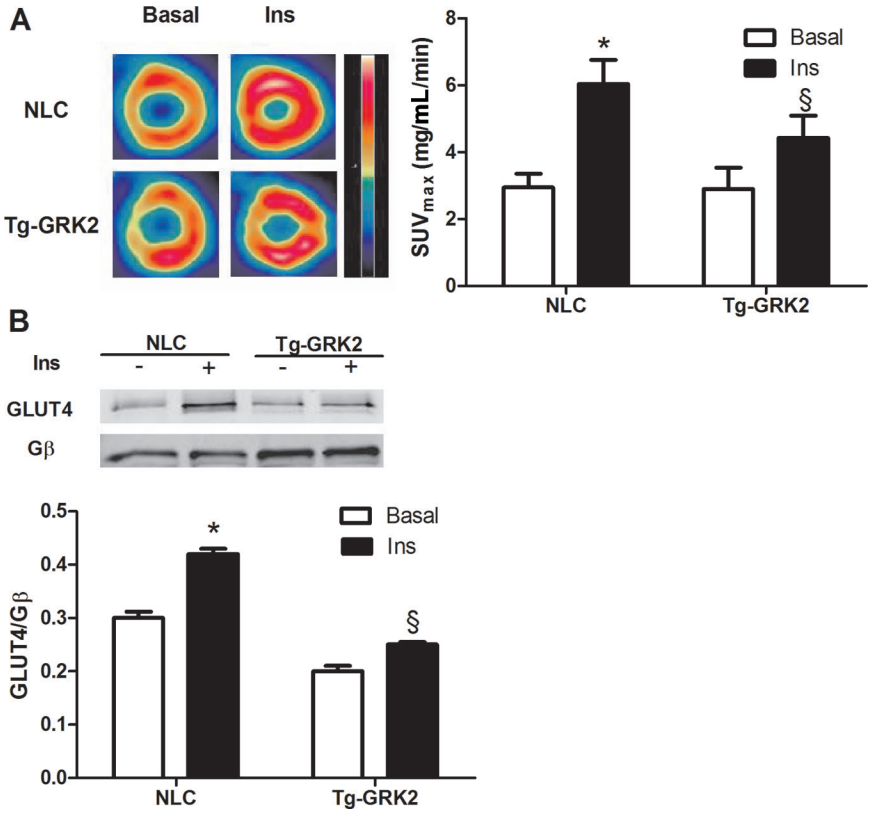

Figure 1. G protein–coupled receptor kinase 2 (GRK2) levels influence in vivo cardiac glucose uptake. **A,** Transgenic (Tg)-GRK2 and nontransgenic littermate control (NLC) mice were studied by positron emission tomography to evaluate cardiac glucose uptake after intraperitoneal injection of insulin (Ins; 0.075 U/kg IP). Insulin significantly increases glucose uptake; however, this response was attenuated in BK12 mice (*$P<0.05$, Ins vs basal; §$P<0.05$, Tg-GRK2 vs NLC; n=8 per group). SUV indicates standardized uptake values. **B,** Plasma membrane GLUT4 protein levels from Tg-GRK2 and NLC hearts. Animals were injected with Ins as above and euthanized 15 minutes later. The GLUT4 levels on the plasma membrane were increased by Ins in NLC but attenuated in Tg-GRK2. The GLUT4 level was normalized to the membrane protein Gβ (*$P<0.05$, Ins vs basal; §$P<0.05$, fold of increased translocation to the membrane, Tg-GRK2 vs NLC; n=3 per group).

dependent on Gαq/11 signaling,[25] and GRK2 has a known RGS domain within its aminoterminus that can interact directly with Gαq and inhibit its activity. Furthermore, GRK2 has recently been shown to interact with and inhibit Akt in endothelial cells.[31] We conducted experiments to test these possible mechanisms and found no evidence that GRK2 interacted with either of these proteins in ARVMs, either basally or after stimulation of cells with insulin (data not shown). Therefore, we explored the possibility that GRK2 could regulate insulin signaling in cardiomyocytes in other ways. Of note, kinase activity of GRK2 was necessary for the negative regulation of insulin signaling because the kinase-dead (K220R) GRK2 dominant-negative mutant (GRK2DN) failed to alter Akt activation (Figure 4A) and GLUT4 membrane translocation in response to insulin (Figure 4B).

We next focused our attention on a potential regulatory role of GRK2 on insulin receptor substrate-1 (IRS1). This molecule moves to the plasma membrane after insulin stimulation and binds activated insulin receptors, leading to Tyr phosphorylation and subsequent activation of downstream signaling.[21] The association of IRS1 with the insulin receptor also initiates events that lead to the attenuation of the

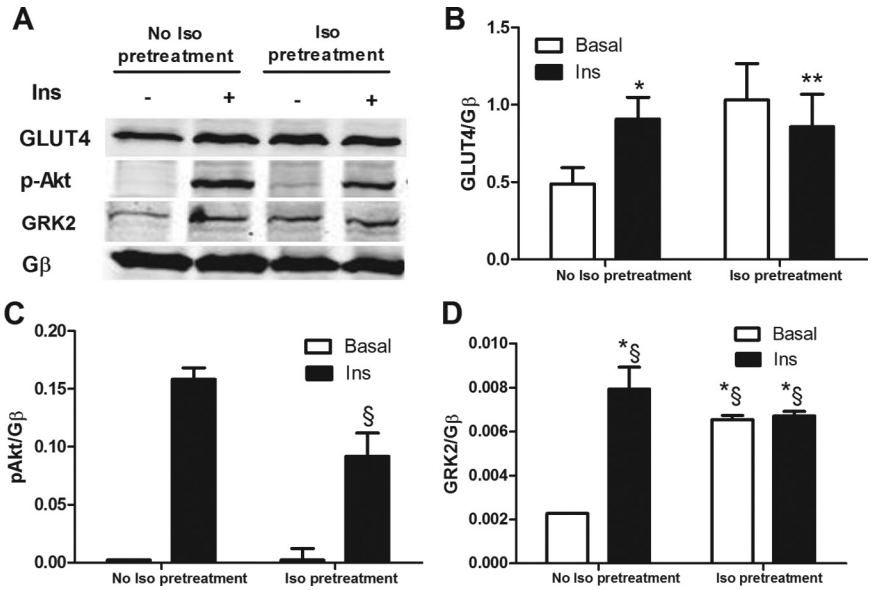

Figure 2. Interplay between β-adrenergic receptor (βAR and insulin receptor signaling. Adult rat ventricular cardiomyocytes were stimulated with insulin (Ins; 0.1 μmol/L for 10 minutes) with or without pretreatment with the βAR agonist isoproterenol (Iso; 10 μmol/L for 5 minutes). Membrane fractions were prepared and blotted for signaling proteins. **A,** Representative Western blot showing membrane GLUT4, phosphorylated (p) Akt, and G protein–coupled receptor kinase 2 (GRK2). Gβ blotting was used as loading control. **B** through **D,** Bar graphs showing GLUT4 translocation (*$P<0.05$, Ins vs basal; n=3; **P=NS, Iso+Ins vs Iso; n=3 per group). Akt was activated in response to Ins but attenuated with Iso pretreatment (§$P<0.05$, fold activation, Iso+Ins vs Ins alone; n=3 per group) and GRK2 translocation induced by Ins with or without Iso pretreatment (*§$P<0.05$, Ins, Iso, and Iso+Ins vs basal; n=3 per group).

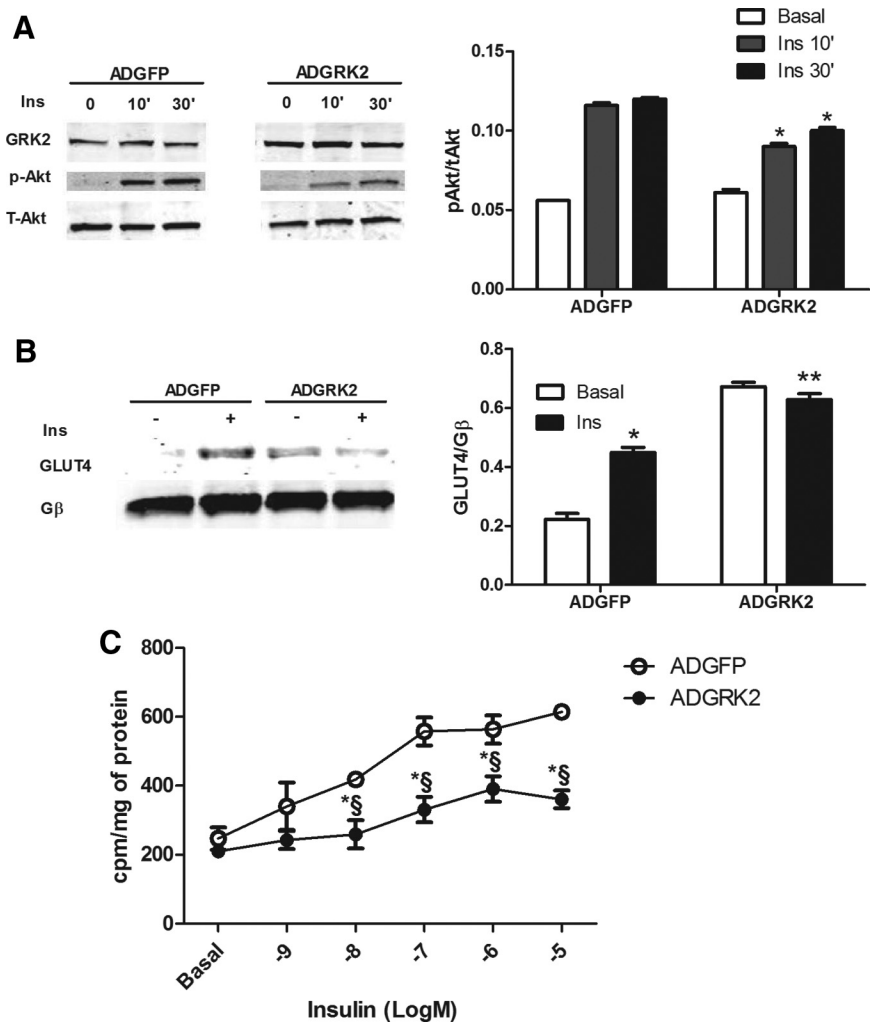

Figure 3. G protein–coupled receptor kinase 2 (GRK2) overexpression in adult rat ventricular cardiomyocytes (ARVMs) inhibits cellular effects of insulin. Adenovirus-infected ARVMs were treated with or without 0.1 μmol/L insulin (Ins) for either 10 or 30 minutes. **A,** Representative Western blot from ARVM whole lysate. Insulin activation of Akt was attenuated by GRK2 overexpression. Total Akt was blotted as loading control (*$P<0.05$, fold activation vs adenovirus [AD] green fluorescent protein [GFP]; n=3 per group). **B,** Western blot from plasma membranes of ARVMs showing increased GLUT4 translocation in response to 0.1 μmol/L Ins for 10 minutes with GFP overexpression but blunted with GRK overexpression (*$P<0.05$ vs basal; **P=NS vs basal; n=3). Gβ was used as loading control. **C,** ARVMs were stimulated with Ins at concentrations ranging from 1 nmol/L to 10 μmol/L for 10 minutes in the presence of ADGFP or ADGRK2 infection. The rate of glucose uptake was determined by [H^3]-deoxyglucose (*§$P<0.01$ vs ADGFP; n=3 per group).

biological effects of insulin[32] through phosphorylation of IRS1 at Ser307, which disrupts IRS1 binding to the insulin receptor and promotes its proteasomal degradation.[33] Of note, when IRS1 is phosphorylated at Ser307, there is a reduction in Tyr612 phosphorylation, and there appears to be a reciprocal relationship between these 2 sites of posttranslational modification.[24,33] A recent study has shown a physical interaction between GRK2 and IRS1 in adipocytes and muscle cells under basal conditions, which is disrupted by insulin treatment.[34] However, our experiments in adult cardiac myocytes show that both GRK2 and IRS1 translocate to the plasma membrane. Moreover, they associate together, and this interaction increases on insulin treatment of myocytes (Figure IA and IB in the online-only Data Supplement). Therefore, we pursued the hypothesis that increased GRK2 activity might enhance the feedback loop induced by insulin via IRS1 inhibitory phosphorylation. We observed that overexpression of GRK2 itself significantly increased Ser307 phosphorylation of IRS1 under basal conditions and after insulin treatment compared with ADGFP-infected cells (Figure 4C).

To address this potential specific role of GRK2 in myocyte insulin signaling, we studied levels of phospho-Ser307 IRS1 in isolated cells from NLC, Tg-GRK2, and cardiac-specific GRK2 knockout (KO) mice[27] after insulin administration. Figure 4D shows that increased cardiac GRK2 in Tg-GRK2 ARVMs results in increased basal and insulin-stimulated IRS1 phospho-Ser307 levels, whereas GRK2KO myocytes have attenuated insulin-stimulated phosphorylation of IRS1 at Ser307 compared with NLC myocytes. Importantly, an in vitro kinase assay shows that purified GRK2 directly phosphorylates purified GST-IRS1 at Ser307 (Figure 4E). The physiological relevance of GRK2 phosphorylation of Ser307 in insulin signaling regulation was explored by using an IRS1 in which Ser307 was mutated to alanine, which could not be phosphorylated by GRK2 (Figure IC in the online-only Data Supplement). Overexpression of this mutated IRS1 by adenovirus (ADIRS1mt) in neonatal rat ventricular cardiomyocytes removes the ADGRK2 inhibitory effects on insulin-mediated activation of Akt (Figure 4F) and GLUT4 translocation to the membrane (Figure ID in the online-only Data Supplement).

Consistent with GRK2 activity inducing Ser307 phosphorylation of IRS1, an inhibitory phosphorylation, we found that GRK2, but not the kinase-dead GRK2 mutant (K220R), also reduced the stimulatory-signaling Tyr612 phosphorylation in ARVMs (Figure IE in the online-only Data Supplement).

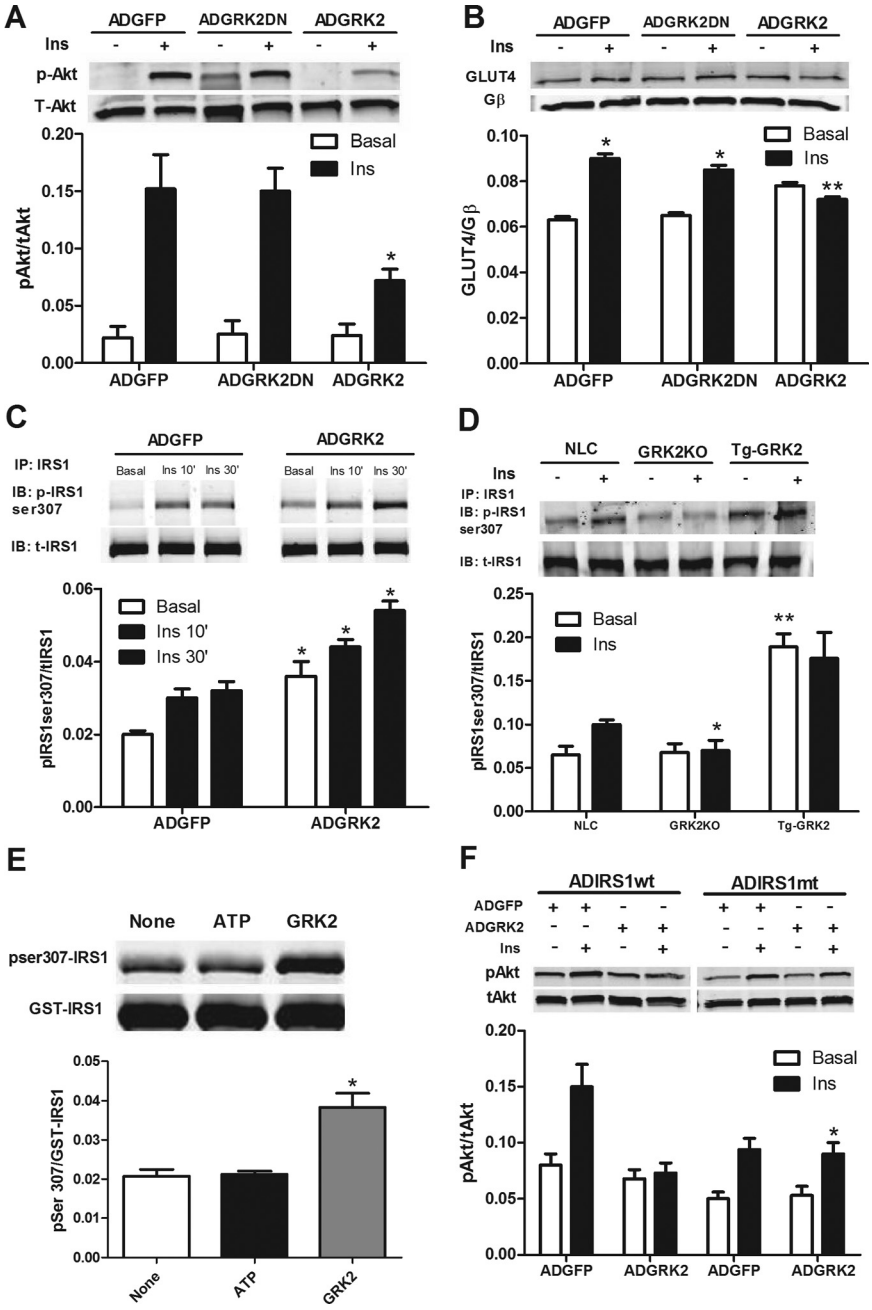

Figure 4. Mechanism of inhibitory effects of G protein–coupled receptor kinase 2 (GRK2) on insulin signaling in myocytes. **A** and **B,** **A**dult rat ventricular cardiomyocytes (ARVMs) were infected with adenovirus (AD) green fluorescent protein (GFP), ADGRK2, or kinase-dead GRK2 (ADGRK2DN) and stimulated with insulin (Ins; 0.1 μmol/L for 10 minutes). **A,** Representative immunoblot (IB) in whole-cell lysates showing reduced phosphorylated (p) Akt levels when GRK2 is overexpressed (*P<0.01, fold activation vs ADGFP and ADGRK2DN; n=3 per group). **B,** Insulin-stimulated GLUT4 membrane levels in ARVMs are attenuated with GRK2 overexpression (*P<0.05 vs basal; **P=NS vs basal; n=3). **C,** Insulin receptor substrate-1 (IRS1) was immunoprecipitated (IP) from whole lysate of ARVMs infected with adenovirus (AD) green fluorescent protein (GFP) or G protein-coupled receptor kinase 2 (ADGRK2) and stimulated with insulin (Ins) as above. Top, Representative immunoblot for phosphorylated (p) Ser307 showing increased p-Ser307 with ADGRK2 treatment. Bottom, Total IRS1 (*P<0.05 vs ADGFP; n=3). **D,** Level of p-Ser307 of IRS1 was evaluated by immunoprecipitation of equal amounts of IRS1 from isolated myocytes of nontransgenic littermate controls (NLC), transgenic (Tg)-GRK2, and cardiac GRK2 knockout (KO) mice after stimulation with Ins (10^{-7} mol/L; 10 minutes). Representative blots for GRK2, p-Ser307, IRS1, and total (t) IRS1 are shown. Reduced and increased levels of pSer307IRS1 were observed in GRK2KO and Tg-GRK2, respectively, vs NLC (*P<0.01, fold of activation, GRK2KO vs NLC; n=3; **P<0.01, Tg-GRK2 vs NLC; n=3 per group). **E,** GRK2 phosphorylates IRS1 at Ser307. An in vitro kinase assay was performed with purified GST-IRS1 alone (none) or in the presence of ATP or ATP plus purified GRK2. Representative blot from 3 independent assays (top) and densitometric analysis (bottom) are shown (*P<0.05, fold activation vs ATP and none). **F,** Neonatal rat ventricular cardiomyocytes (NRVMs) were coinfected with either ADIRS1 wild type (wt) or ADIRS1 mutant Ser307Ala (mt) in addition to ADGFP or ADGRK2 and stimulated with Ins as above. Representative immunoblot showing p-Akt levels is provided (*P<0.01, fold activation vs ADGRK2+ADIRS1wt; n=3 per group).

Cardiac Glucose Uptake Defects Precede Heart Failure Development After Myocardial Infarction, and Both Are Augmented With G Protein–Coupled Receptor Kinase 2 Upregulation

With our findings that increased GRK2 levels in myocytes negatively affect insulin signaling, we next sought to determine whether this translates to the pathogenesis of HF. To determine whether GRK2-mediated loss of glucose metabolism occurs in compromised myocardium, we used micro-PET to follow 18-FDG uptake after myocardial infarction (MI). Left coronary artery ligation induced a reproducible LV infarct in Tg-GRK2, GRK2KO, and NLC mice, as previously described[27] (data not shown). All groups showed increased 18-FDG uptake 1 week after MI, consistent with the heart increasing to the more protective glucose metabolism.[5] However, the immediate post-MI glucose uptake response was significantly reduced in Tg-GRK2 mice compared with NLC (Figure 5A). Furthermore, a progressive reduction in glucose uptake after MI is observed in both NLC and Tg-GRK2 mice, which accompanies progressive post-MI cardiac dysfunction and LV remodeling as measured by echocardiography (Figure 5B). In cardiac GRK2KO mice, there was an initial lower glucose uptake response immediately after MI; however, in vivo glucose uptake remained stable throughout the study period, resulting in significantly higher uptake compared with the NLC group at 6 to 8 weeks after MI (Figure 5A). Interestingly, as in ARVMs (Figure 3C), attenuated cardiac glucose uptake in vivo over time was significantly attenuated with GRK2 overexpression, and this worsened metabolic effect was most evident 1 to 3 weeks after MI (Figure 5A). These data show that higher levels of myocardial GRK2 cause immediate post-MI defects in glucose metabolism that are evident before LV dysfunction appears; accordingly, Tg-GRK2 mice have significantly worse cardiac function and remodeling long-term after MI, whereas cardiac GRK2KO mice showed a preserved glucose use, resulting in preserved cardiac volume and function (Figure 5B and 5C).

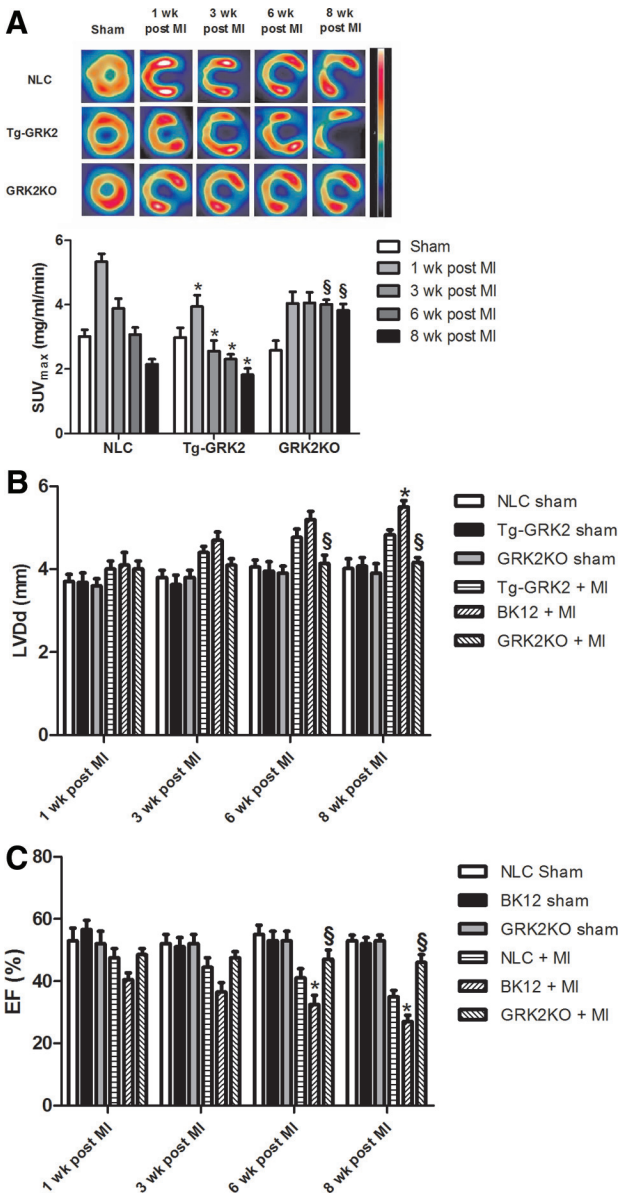

Figure 5. Cardiac glucose uptake in post–myocardial infarction (MI) mice. **A,** 18-Fluorodeoxyglucose (18-FDG) cardiac uptake in nontransgenic littermate control (NLC), transgenic–G protein–coupled receptor kinase 2 (Tg-GRK2), and cardiac-specific GRK2 knockout (KO) mice under sham conditions and 1 to 8 weeks after MI. Top, Representative micro–positron emission tomography images in which the infarct is clearly visible. Bottom, Histogram quantifying 18-FDG uptake in myocardium (*$P<0.05$, Tg-GRK2 vs NLC; § $P<0.05$, GRK2 knockout [lsqb[KO] vs NLC; n=12 per group). SUV indicates standardized uptake values. **B** and **C,** Left ventricular diameter at diastole (LVDd) and ejection fraction (EF) in NLC, Tg-GRK2, and GRK2KO mice determined by echocardiography serially after MI (*$P<0.01$, Tg-GRK2 vs NLC; §$P<0.01$, GRK2KO vs NLC; n=12 per group).

Carboxyl Terminal Domain of G Protein–Coupled Receptor Kinase 2 Improves Insulin Signaling in Adult Cardiomyocytes

Our data indicate that excess GRK2 produces serious modifications in cardiac glucose uptake and insulin signaling in vivo and in vitro. Inhibition of GRK2 activity through the carboxyl terminal domain of GRK2 (βARKct) has previously rescued several models of HF.[21,29] In light of the above data showing, in particular, the protective role of myocardial GRK2 loss on cardiac metabolism, we hypothesized that the beneficial effect of βARKct in rescuing cardiac function during HF could be due, at least in part, to a favorable effect on cardiac metabolism. Indeed, transgenic mice with cardiac βARKct expression (Tg-βARKct) have significantly lower inhibitory IRS1 Ser307 phosphorylation induced by insulin (Figure 6A), similar to data in cardiac-specific GRK2 KO mice (Figure 4D). Therefore, βARKct has the potential to enhance insulin signaling. We tested this hypothesis by introducing βARKct in ARVMs via an adenovirus (ADβARKct). We found that βARKct expression restores and enhances Akt phosphorylation and a downstream target of Akt, GSK3β, compared with levels found in ADGRK2- and ADGFP-treated myocytes, respectively (Figure 6B and 6C).

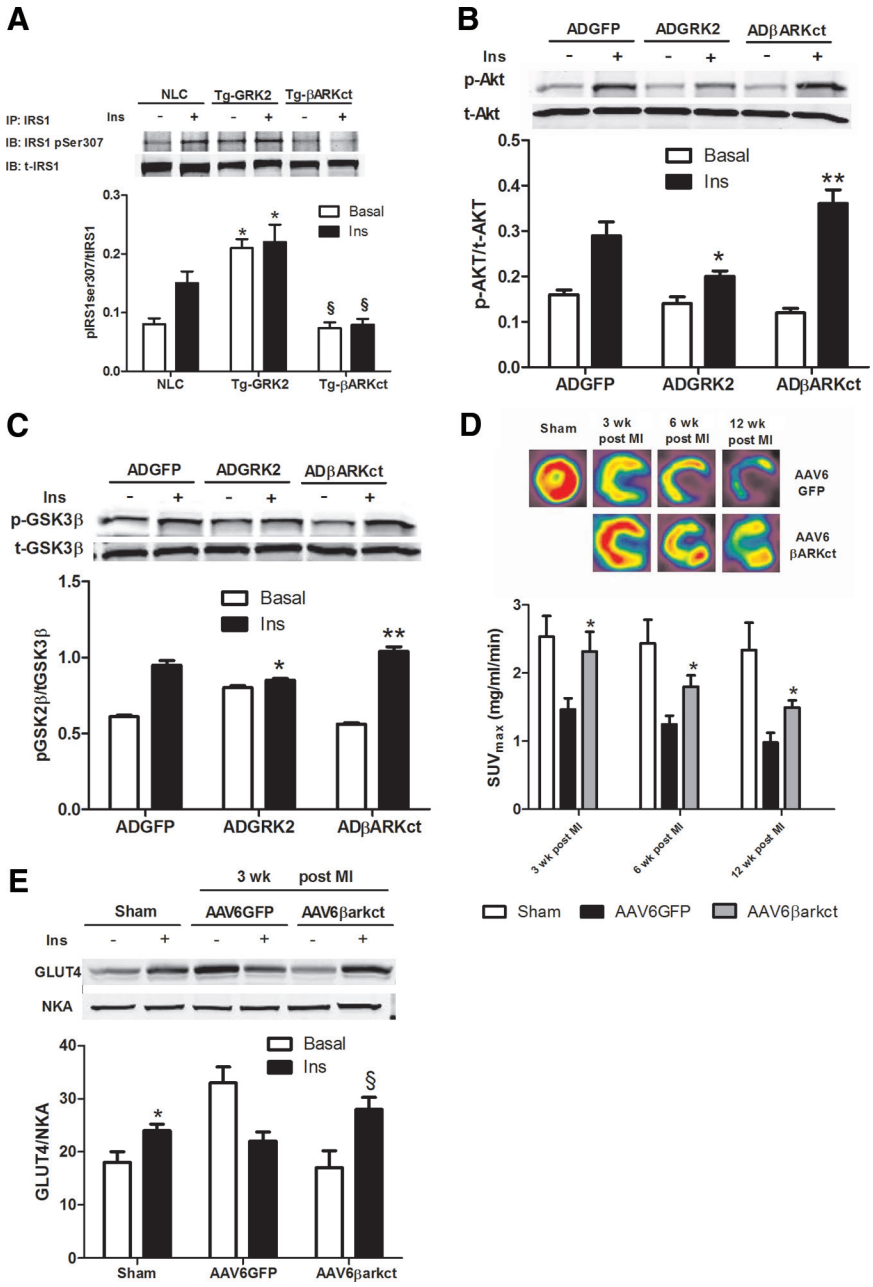

Figure 6. Inhibition of G protein–coupled receptor kinase 2 (GRK2) in myocytes and myocardium restores normal insulin (Ins) signaling and prevents defective in vivo glucose uptake after myocardial infarction (MI). **A,** Level of Ins-stimulated phosphorylated (p) Ser307 in insulin receptor substrate-1 (IRS1) immunoprecipitated (IP) from adult mouse ventricular myocytes isolated from nontransgenic littermate controls (NLC), transgenic (Tg)-GRK2, or Tg–carboxyl terminal domain of GRK2 (Tg-βARKct mice) (*$P<0.01$ vs NLC; n=3; §$P<0.01$, Tg-βARKct vs NLC; n=3 per group). IB indicates immunoblot. **B,** Adult rat ventricular myocytes (ARVMs) were infected with adenovirus (AD) green fluorescent protein (GFP), ADGRK2, or ADβARKct. Representative blots for p-Akt and total (t) Akt are shown (*$P<0.01$, fold increase in activation, ADGRK2 vs ADGFP; n=3; **$P<0.01$, fold increase in activation, ADβARKct vs ADGRK2 and ADGFP; n=3 per group). **C,** Representative Western blot from ARVM whole lysate infected as in **A** and stimulated with Ins showing p-GSK3β and t-GSK3β (*$P<0.01$, fold increase in activation, ADGRK2 vs ADGFP; n=3; **$P<0.01$, fold increase in activation, ADβARKct vs ADGRK2; n=3). **D,** Global rat myocardial in vivo glucose uptake evaluated by micro–positron emission tomography in sham and 1-, 3-, 6-, and 12-week post-MI rats treated with AAV6-GFP or AAV6-βARKct (*$P<0.05$ vs AAV6GFP; n=8 per group). **E,** Rats 3 weeks after MI and sham were euthanized 15 minutes after an intraperitoneal injection of insulin (0.075 U/kg), and hearts were removed. Plasma membranes were prepared to evaluate GLUT4 levels as shown in a representative blot (*$P<0.05$ vs basal; §$P<0.05$ vs basal; n=3 per group).

AAV6–Carboxyl Terminal Domain of G Protein–Coupled Receptor Kinase 2 Gene Therapy Prevents G Protein–Coupled Receptor Kinase 2–Mediated Defects in Cardiac Glucose Metabolism Before the Rescue of Subsequent Heart Failure

Next, we asked whether inhibiting GRK2 could lift the negative effects of this kinase on in vivo myocardial insulin signaling and measured myocardial glucose uptake and insulin responses in post-MI rat hearts that expressed βARKct. To do this, we injected AAV6-GFP or AAV6-βARKct into the myocardium of rats during surgery to induce an MI, as we have done previously.[28] Then, we serially measured in vivo glucose uptake in the heart via micro-PET, along with LV dimension and function via echocardiography and LV catheterization. As expected, our method of cardiac gene transfer led to long-term and robust βARKct expression in the rat heart (Figure IIA in the online-only Data Supplement). AAV6-βARKct delivery compared with AAV6-GFP did not produce any significant differences in cardiac function and volume in sham-treated rats (data not shown); therefore, in our data presentation, we show only 1 sham control group.

MI induces progressive dilatation and LV dysfunction (Figure IIC and IID and Table I in the online-only Data Supplement), and consistent with human and animal models of HF, we found a progressive increase in myocardial GRK2 levels after MI (Figure IIB in the online-only Data Supplement). Rats treated with AAV6-βARKct had significantly improved post-MI cardiac function and significantly less remodeling throughout the 12 weeks of study (Figure IIC and IID and Table I in the online-only Data Supplement) with respect to the AAV6-GFP group. When we assessed in vivo

glucose uptake after MI via micro-PET, we found that MI caused an immediate defect in 18-FDG uptake in control AAV6-GFP–treated rats; this metabolic abnormality was evident before any cardiac dysfunction or remodeling was found (Figure 6D), a finding that was similar to the above studies in mice (Figure 5). Interestingly, AAV6-βARKct–treated rats actually had normal myocardial glucose uptake 3 weeks after MI, and this was significantly improved over post-MI GFP-treated rats throughout the study (Figure 6D). To evaluate the potential in vivo mechanism of the above PET results, we took a cohort of 3-week post-MI rats and challenged them with insulin to measure GLUT4 membrane localization and found this to be significantly blunted in GFP-treated rats. However, AAV6-βARKct–treated animals had significantly improved insulin responsiveness (Figure 6E).

Discussion

Our findings add significantly to the dynamic role of GRK2 in the pathogenesis of HF in that they uncover a new mechanism by which upregulated GRK2 in the injured myocardium promotes ventricular dysfunction. Importantly, enhanced GRK2 activity not only negatively affects cardiac contractile function after myocardial injury, but also causes abnormal cardiac metabolism. Furthermore, GRK2 may represent a molecular link between the excessive neurohormonal activation that follows cardiac stress and initiation of defects in myocyte energy substrate use. Of note, our data reveal that GRK2 inhibition via βARKct expression or its gene deletion in myocytes corrects metabolic alterations observed during the early stages of postischemic HF. This facilitates myocyte use of glucose, which is a protective metabolic substrate, and delays the development of HF.

As observed in our micro-PET studies, the modification in cardiac glucose uptake is an early event after the induction of MI. In particular, the initial increase is followed by a progressive reduction, which is then accompanied by a progressive cardiac dilation and reduced function. This behavior observed in NLC mice is significantly modified in mice with altered GRK2 levels in myocytes. Enhanced GRK2 cardiac expression in Tg-GRK2 mice significantly reduces protective myocyte glucose uptake, whereas cardiac-targeted GRK2KO mice have preserved glucose uptake throughout the 8-week post-MI period. Given the higher efficiency of glucose in ATP production and the lower impact in oxidative stress with respect to other substrates, we show that GRK2-mediated pathogenesis in HF is mediated, at least in part, through negative alterations in cardiac metabolism.

Our findings once again highlight the deleterious effects of increased GRK2 levels that accompany myocardial ischemia, and, most important, confirm the importance of identifying strategies aimed specifically to reduce its activity in the heart as potential HF therapy. Moreover, GRK2 inhibition with βARKct, which has been demonstrated to rescue or prevent animal models of HF and to improve contractile function of failing human ventricular myocytes,[28,35] has beneficial effects that extend beyond the functional recovery of βARs and contractility. Indeed, previous studies showed that GLUT4 overexpression improves cardiac function in mice with cardiac insulin resistance.[14,15] We demonstrate here that lowering GRK2 during HF improves glucose uptake and delays the development of the disease. We attribute at least part of the improvement to restored insulin-stimulated GLUT4 membrane translocation. G protein–coupled receptor kinase 2 also represents the first identification of a molecule that represents a nodal link between excessive neurohormonal stimulation and metabolic abnormalities, supporting the hypothesis that strategies aimed to preserve myocardial metabolism could be beneficial in the treatment or prevention of HF.

Insulin signaling is known to be protective in the heart by inhibiting apoptosis and oxidative stress[36]; it is also an important regulator of cardiac mass.[37] These effects are mediated primarily by activation of PI3K-Akt and inhibition of GSK3β.[38] On the basis of the results of this study, injury-induced increases in GRK2 within the cardiomyocyte may increase oxidative stress, which expands our mechanistic understanding of why Tg-GRK2 mice progress more rapidly to HF. Therefore, GRK2 clearly has effects in the myocyte that extend beyond G protein–coupled receptor–mediated functions, improving our mechanistic understanding of the pathological nature of GRK2 in the heart.

Of interest, recent studies have described a correlation between insulin resistance and increased levels of GRK2 in pathological conditions. In particular, Garcia-Guerra et al[34] have recently found that overexpression of either GRK2 or the kinase-dead mutant reduces insulin sensitivity in myoblasts and adipocytes, and that finding was consistent with other studies[25,31] that suggested that a kinase-independent mechanism was involved, possibly by sequestering molecules involved in insulin signaling such as Gαq/11, Akt, and IRS1. However, our data demonstrate for the first time that the catalytic activity of GRK2 is fundamental and a requirement in postischemic cardiac metabolic alterations, in particular, the dampening insulin signaling.

The finding that Ser307 of IRS1 is a target for GRK2 phosphorylation in cardiomyocytes significantly increases the overall knowledge about the regulation of insulin signaling in physiology and pathology. Several serine residues within IRS1 are involved in the physiological mechanism of IRS1 inhibition; however, Ser307 has specific properties and characteristics that make it particularly interesting as a target of GRK2. This site is found proximal to the IRS1 phospho-Tyr binding domain, and Ser307 phosphorylation rapidly reduces its affinity for binding to the insulin receptor,[33] a process that resembles βAR desensitization. Thus, GRK2 appears to directly modulate signaling through this non–G protein–coupled receptor and participates in the physiological regulation of insulin signaling. Accordingly, GRK2 inhibition reduces insulin-mediated Ser307 phosphorylation and improves signaling, and as a result can improve glucose uptake and insulin resistance in the injured cardiomyocyte. Indeed, elevated levels of phospho-Ser307 of IRS1 have been observed in animal models of insulin resistance, and the equivalent Ser312 site in human IRS1 has been demonstrated to be hyperphosphorylated in insulin-resistant subjects.[39,40] Therefore, our findings can hypothetically be extended beyond the heart, and suggest that βARKct gene therapy could be used for the possible treatment of reduced skeletal muscle

and liver glucose uptake, as is observed in type II diabetes mellitus.

Overall, our data show that GRK2 inhibition clearly delays the reduction in glucose uptake and protects insulin signaling in the heart, preserving cardiac dimension and function. These data support the novel hypothesis that part of the therapeutic effect of GRK2 inhibition in HF includes correction of abnormal cardiac metabolism.

Acknowledgments

We thank Dr M. Thakur and K. Devadalas of the Jefferson PET core facility for conducting the PET imaging and analyzing the micro-PET data. We also thank Filomena Severino and Dr Daniela Femminella for their technical support and encouragement.

Sources of Funding

This work was supported in part by US National Institutes of Health grants R01 HL085503, R37 HL61690, and P01 HL075443 (project 2; to Dr Koch) and a fellowship from the Great Rivers Affiliate of the American Heart Association (to Dr Ciccarelli).

Disclosures

None.

References

1. Braunwald E. The Denolin Lecture: congestive heart failure: a half century perspective. *Eur Heart J*. 2001;22:825–836.
2. Jessup M, Brozena S. Heart failure. *N Engl J Med*. 2003;348:2007–2018.
3. Neubauer S. The failing heart: an engine out of fuel. *N Engl J Med*. 2007;356:1140–1151.
4. Ingwall JS, Weiss RG. Is the failing heart energy starved? On using chemical energy to support cardiac function. *Cir Res*. 2004;95:135–145.
5. Ashrafian H, Frenneaux MP. Metabolic modulation in heart failure: the coming of age. *Cardiovasc Drugs Ther*. 2007;21:5–7.
6. Bing RJ, Siegel A, Ungar I, Gilbert M. Metabolism of the human heart, II: studies on fat, ketone, and amino acid metabolism. *Am J Med*. 1954; 16:504–515.
7. Wisneski JA, Gertz EW, Neese RA, Mayr M. Myocardial metabolism of free fatty acids: studies with 14C-labeled substrates in humans. *J Clin Invest*. 1987;79:359–366.
8. Lommi J, Kupari M, Yki-Jarvinen H. Free fatty acid kinetics and oxidation in congestive heart failure. *Am J Cardiol*. 1998;81:45–50.
9. Taylor M, Wallhaus TR, Degrado TR, Russell DC, Stanko P, Nickles RJ, Stone CK. An evaluation of myocardial fatty acid and glucose uptake using PET with [18F]fluoro-6-thia-heptadecanoic acid and [18F]FDG in patients with congestive heart failure. *J Nucl Med*. 2001;42:55–62.
10. Horn M, Remkes H, Stromer H, Dienesch C, Neubauer S. Chronic phosphocreatine depletion by the creatine analogue beta-guanidinopropionate is associated with increased mortality and loss of ATP in rats after myocardial infarction. *Circulation*. 2001;104:1844–1849.
11. Neubauer S, Krahe T, Schindler R, Horn M, Hillenbrand H, Entzeroth C, Mader H, Kromer EP, Riegger GA, Lackner K. 31P magnetic resonance spectroscopy in dilated cardiomyopathy and coronary artery disease: altered cardiac high-energy phosphate metabolism in heart failure. *Circulation*. 1992;86:1810–1818.
12. Peterson LR, Waggoner AD, Schechtman KB, Meyer T, Gropler RJ, Barzilai B, Davila-Roman VG. Alterations in left ventricular structure and function in young healthy obese women: assessment by echocardiography and tissue Doppler imaging. *J Am Coll Cardiol*. 2004;43:1399–1404.
13. Mazumder PK, O'Neill BT, Roberts MW, Buchanan J, Yun UJ, Cooksey RC, Boudina S, Abel ED. Impaired cardiac efficiency and increased fatty acid oxidation in insulin-resistant ob/ob mouse hearts. *Diabetes*. 2004; 53:2366–2374.
14. Belke DD, Larsen TS, Gibbs EM, Severson DL. Altered metabolism causes cardiac dysfunction in perfused hearts from diabetic (db/db) mice. *Am J Physiol Endocrinol Metab*. 2000;279:E1104–E1113.
15. Semeniuk LM, Kryski AJ, Severson DL. Echocardiographic assessment of cardiac function in diabetic db/db and transgenic db/db-hGLUT4 mice. *Am J Physiol Heart Circ Physiol*. 2002;283:H976–H982.
16. Boudina S, Bugger H, Sena S, O'Neill BT, Zaha VG, Ilkun O, Wright JJ, Mazumder PK, Palfreyman E, Tidwell TJ, Theobald H, Khalimonchuk O, Wayment B, Sheng X, Rodnick KJ, Centini R, Chen D, Litwin SE, Weimer BE, Abel ED. Contribution of impaired myocardial insulin signaling to mitochondrial dysfunction and oxidative stress in the heart. *Circulation*. 2009;119:1272–1283.
17. Witteles RM, Tang WH, Jamali AH, Chu JW, Reaven GM, Fowler MB. Insulin resistance in idiopathic dilated cardiomyopathy: a possible etiologic link. *J Am Coll Cardiol*. 2004;44:78–81.
18. Kostis JB, Sanders M. The association of heart failure with insulin resistance and the development of type 2 diabetes. *Am J Hypertens*. 2005;18:731–737.
19. Zucker IH. Novel mechanisms of sympathetic regulation in chronic heart failure. *Hypertension*. 2006;48:1005–1011.
20. Opie LH, Thandroyen FT, Muller C, Bricknell OL. Adrenaline-induced "oxygen-wastage" and enzyme release from working rat heart: effects of calcium antagonism, beta-blockade, nicotinic acid and coronary artery ligation. *J Mol Cell Cardiol*. 1979;11:1073–1094.
21. Iaccarino G, Koch WJ. Transgenic mice targeting the heart unveil G protein-coupled receptor kinases as therapeutic targets. *Assay Drug Dev Technol*. 2003;1:347–355.
22. Iaccarino G, Barbato E, Cipolletta E, De Amicis V, Margulies KB, Leosco D, Trimarco B, Koch WJ. Elevated myocardial and lymphocyte GRK2 expression and activity in human heart failure. *Eur Heart J*. 2005;26:1752–1758.
23. Bonita RE, Raake PW, Otis NJ, Chuprun JK, Spivack T, Dasgupta A, Whellan DJ, Mather PJ, Koch WJ. Dynamic changes in lymphocyte GRK2 levels in cardiac transplant patients: a biomarker for left ventricular function. *Clin Transl Sci*. 2008;3:14–18.
24. Shahid G, Hussain T. GRK2 negatively regulates glycogen synthesis in mouse liver FL83B cells. *J Biol Chem*. 2007;282:20612–20620.
25. Usui I, Imamura T, Babendure JL, Satoh H, Lu JC, Hupfeld CJ, Olefsky JM. G protein-coupled receptor kinase 2 mediates endothelin-1-induced insulin resistance via the inhibition of both Galphaq/11 and insulin receptor substrate-1 pathways in 3T3–L1 adipocytes. *Mol Endocrinol*. 2005;19:2760–2768.
26. Cipolletta E, Campanile A, Santulli G, Sanzari E, Leosco D, Campiglia P, Trimarco B, Iaccarino G. The G protein coupled receptor kinase 2 plays an essential role in beta-adrenergic receptor-induced insulin resistance. *Cardiovasc Res*. 2009;84:407–415.
27. Raake PW, Vinge LE, Gao E, Boucher M, Rengo G, Chen X, DeGeorge BR Jr, Matkovich S, Houser SR, Most P, Eckhart AD, Dorn GW 2nd, Koch WJ. G protein-coupled receptor kinase 2 ablation in cardiac myocytes before or after myocardial infarction prevents heart failure. *Circ Res*. 2008;103:413–422.
28. Rengo G, Lymperopoulos A, Zincarelli C, Donniacuo M, Soltys S, Rabinowitz JE, Koch WJ. Myocardial adeno-associated virus serotype 6-betaARKct gene therapy improves cardiac function and normalizes the neurohormonal axis in chronic heart failure. *Circulation*. 2009;119:89–98.
29. Rockman HA, Koch WJ, Lefkowitz RJ. Seven-transmembrane-spanning receptors and heart function. *Nature*. 2002;415:206–212.
30. Koch WJ, Rockman HA, Samama P, Hamilton RA, Bond RA, Milano CA, Lefkowitz RJ. Cardiac function in mice overexpressing the beta-adrenergic receptor kinase or a beta ARK inhibitor. *Science*. 1995;268: 1350–1353.
31. Liu S, Premont RT, Kontos CD, Zhu S, Rockey DC. A crucial role for GRK2 in regulation of endothelial cell nitric oxide synthase function in portal hypertension. *Nat Med*. 2005;11:952–958.
32. Sun XJ, Goldberg JL, Qiao LY, Mitchell JJ. Insulin-induced insulin receptor substrate-1 degradation is mediated by the proteasome degradation pathway. *Diabetes*. 1999;48:1359–1364.
33. Aguirre V, Werner ED, Giraud J, Lee YH, Shoelson SE, White MF. Phosphorylation of Ser307 in insulin receptor substrate-1 blocks interactions with the insulin receptor and inhibits insulin action. *J Biol Chem*. 2002;277:1531–1537.
34. Garcia-Guerra L, Nieto-Vazquez I, Vila-Bedmar R, Jurado-Pueyo M, Zalba G, Diez J, Murga C, Fernandez-Veledo S, Mayor F Jr, Lorenzo M. G protein-coupled receptor kinase 2 (Grk2) plays a relevant role in insulin resistance and obesity. *Diabetes*. 2010;59:2407–2417.
35. Williams ML, Hata JA, Schroder J, Rampersaud E, Petrofski J, Jakoi A, Milano CA, Koch WJ. Targeted beta-adrenergic receptor kinase (betaARK1) inhibition by gene transfer in failing human hearts. *Circulation*. 2004;109: 1590–1593.
36. Aikawa R, Nawano M, Gu Y, Katagiri H, Asano T, Zhu W, Nagai R, Komuro I. Insulin prevents cardiomyocytes from oxidative stress-induced

apoptosis through activation of PI3 kinase/Akt. *Circulation*. 2000;102:2873–2879.
37. Decker RS, Cook MG, Behnke-Barclay M, Decker ML. Some growth factors stimulate cultured adult rabbit ventricular myocyte hypertrophy in the absence of mechanical loading. *Circ Res*. 1995;77:544–555.
38. Markou T, Cullingford TE, Giraldo A, Weiss SC, Alsafi A, Fuller SJ, Clerk A, Sugden PH. Glycogen synthase kinases 3alpha and 3beta in cardiac myocytes: regulation and consequences of their inhibition. *Cell Signal*. 2008;20:206–218.
39. Werner ED, Lee J, Hansen L, Yuan M, Shoelson SE. Insulin resistance due to phosphorylation of insulin receptor substrate-1 at serine 302. *J Biol Chem*. 2004;279:35298–35305.
40. Morino K, Petersen KF, Dufour S, Befroy D, Frattini J, Shatzkes N, Neschen S, White MF, Bilz S, Sono S, Pypaert M, Shulman GI. Reduced mitochondrial density and increased IRS-1 serine phosphorylation in muscle of insulin-resistant offspring of type 2 diabetic parents. *J Clin Invest*. 2005;115:3587–3593.

CLINICAL PERSPECTIVE

A large number of studies have demonstrated that the increased level of G protein–coupled receptor kinase 2 (GRK2) seen in injured myocardium has deleterious effects on the progression of heart failure (HF). Importantly, GRK2 lowering is associated with improved cardiomyocyte signaling and function in failing human hearts mechanically unloaded with assist devices. However, the mechanisms through which GRK2 promotes HF, or why its inhibition is therapeutic has not been fully elucidated. Interestingly, therapies targeting the neurohormonal axis, such as β-blockers, can attenuate cardiac remodeling and improve prognosis in patients with HF, and these drugs can significantly decrease GRK2 in the heart. On the other hand, agents aimed at directly increasing cardiac contractility have failed. Thus, it appears that GRK2 lowering and inhibition, which improve contractility, must have additional effects on pathological components of HF development to account for the overwhelming positive effects seen in various animal models. The present study provides the first evidence that there is a close relationship between GRK2 activity and unfavorable modifications of cardiac metabolism, including insulin resistance and a loss of glucose uptake that can occur after ischemic injury and through the progression to HF. Indeed, we have identified IRS1 as a novel substrate of GRK2 kinase activity that can attenuate insulin signaling in the myocyte. These data also demonstrate that insulin resistance and defective glucose uptake appear in the early stages of HF, suggesting the use of therapies aimed at restoring correct metabolic substrate utilization in the myocyte as soon as possible after ischemic injury. In this scenario, lowering GRK2, which is known to be upregulated acutely after myocardial injury, appears to be a feasible and exciting approach to maintain metabolic homeostasis in the myocyte, which may contribute significantly to preventing the development of subsequent ischemic HF.

G Protein–Coupled Receptor Kinase 2 Activity Impairs Cardiac Glucose Uptake and Promotes Insulin Resistance After Myocardial Ischemia

Michele Ciccarelli, J. Kurt Chuprun, Giuseppe Rengo, Erhe Gao, Zhengyu Wei, Raymond J. Peroutka, Jessica I. Gold, Anna Gumpert, Mai Chen, Nicholas J. Otis, Gerald W. Dorn II, Bruno Trimarco, Guido Iaccarino and Walter J. Koch

Circulation. 2011;123:1953-1962; originally published online April 25, 2011;
doi: 10.1161/CIRCULATIONAHA.110.988642
Circulation is published by the American Heart Association, 7272 Greenville Avenue, Dallas, TX 75231

Print ISSN: 0009-7322. Online ISSN: 1524-4539

GRK2 Activity Impairs Cardiac Glucose Uptake and Promotes Insulin Resistance Following Myocardial Ischemia

SUPPLEMENTAL MATERIAL

Supplementary Methods

Isolation and adenoviral infection of ventricular cardiomyocytes for *in vitro* experiments. Adult rat ventricular myocytes **(**ARVMs) and adult mouse ventricular myocytes (AMVMs) were isolated from 12 week old Sprague/Dawley rat or mouse hearts, respectively, by a standard enzymatic digestion procedure and cultivated as described [1]. Rat neonatal ventricular myocytes (NRVMs) were isolated as previously described [2]. Adult and neonatal myocytes were treated with various adenoviruses as previously described [2]. Cells were generally used for experiments 48hrs post infection.

Surgical induction of MI. All animal procedures and experiments were performed in accordance with the guidelines of the Institutional Animal Care and Use Committee of Thomas Jefferson University. Mice at 8-10 weeks of age were used for MI experiments in which left anterior descending (LAD) coronary artery ligation was carried as described previously [3, 4]. For rat MI, 12 week old Sprague/Dawley rats were used and a previously described model of cryoinfarction was used [5]. Briefly, anesthetized adult male (175-200g) rats were intubated and mechanically ventilated and anesthesia was maintained using a 2% isoflurane (v/v) oxygen mixture. Cryothermia was applied by use of three freeze cycles of 1 min each that was interrupted by one minute thawing intervals. Soon after induction of MI, myocardial gene transfer was achieved by intra-myocardial direct injection as previously described [5].

***In vivo* cardiac glucose uptake measurement by microPET.** Imaging was performed in the prone position using an animal microPET scanner (Inveon Dedicated PET, Siemens Medical Solutions Inc). Animals were starved 2 hrs before the study to normalize glucose and insulin

levels and anesthetized using 1.5% isoflurane throughout the imaging. After starting image acquisition, animals were injected with an average of 30 MBq of 18 FluorDeoxyGlucose (18-FDG) in the tail vein. The dynamic PET acquisition continued for 120 minutes in listmode format. Images were reconstructed as previously described [6]. FDG uptake in the myocardium was semiquantitatively assessed by evaluating the standardized uptake value (SUV, activity concentration/injected dose/body weight). Regions of interest (ROI) were obtained by drawing area of equal size on the myocardium by excluding the infarcted and non uptake area and SUV calculated from an averaged image of the last 30 min (6 frames) of the FDG scan using the following equation: voxel value within ROI (Mbq/ml)/activity injected (Mbq)/body weight (mg). Data are expressed as maximal value of SUV in the last 30 min of scanning (SUV_{max}).

Glucose uptake in ARVMs. Glucose uptake assay was performed as previously described with some modifications [7]. Assays were performed in triplicate in 12-well (22 mm in diameter) laminin-coated tissue culture plates. Cells were washed twice with 1 ml of glucose-free DMEM and then 1 ml of glucose-free DMEM (37 °C) containing insulin or PBS, 1 mM pyruvate and 0.1% BSA was added. 40 min later 10 µl of a 2-deoxyglucose mix containing 130 µl of glucose-free DMEM, 15 µl of 100-mM 2-deoxyglucose solution, and 5 µl of 1µCi/µl [^{3}H]2-deoxyglucose was added. After 30 min the cells were lysed in 500 µl of NaOH (1 M) for 20 min at 37 °C. A 400-µl aliquot of the lysed extract was counted to determine the specific activity of [^{3}H] 2-deoxyglucose and normalized the result to protein concentration (Pierce). Data were expressed as cpm/mg of protein.

***In-vitro* kinase assay using FLAG-IRS1**. NRVMs were infected using adenovirus encoding for the expression of either Flag-tagged wild-type IRS1 or the IRS1-S307A mutant. IRS1 was immunopreciptated from whole cell lysates using a Flag antibody conjugated to agarose beads (Sigma). Equal amounts of wild-type or mutant IRS1 were used as substrate in the in-vitro kinase assay. Phosphorylation reactions were conducted in a 50ul reaction volume in kinase buffer that contained 25mM Tris (pH7.5), 10mM $MgCl_2$, 2mM DTT, 5mM α-Glycerophosphate, and 0.1mM Na_3VO_4 and 0.2mM ATP. GRK2-stimulated phosphorylation was initiated by the addition of 250ng purified GRK2 (Invitrogen) and 100ng Gβγ subunits (Calbiochem). Reactions were carried out for 30min at 30^{o}C and stopped by the addition of 50ul of 2x sample loading dye. Samples were heated for 5 min at 95^{o}C, mixed and briefly centrifuged to pellet the flag beads. 30ul of each reaction was loaded onto a 4-20% Tris-Glycine gel and following electrophoresis the proteins were transferred to nitrocellulose for western blotting. The phosphorylation state of IRS1 was probed using a site specific antibody to Ser307 (Millipore) and the amount of total IRS1 used in the assay was detected by blotting for Flag (Sigma). For quantification the amount of phosho-Ser307 was normalized to total IRS1 for a given reaction.

In-vitro Kinase Assay using purified GST-IRS1. A GST-IRS1 fusion protein consisting of mouse IRS1 amino acid residues 108-516 was used as the substrate for reconstitution kinase assays. This murine IRS1 fragment (108-516) was amplified by PCR and subcloned into pGEX-2T using standard molecular biological techniques and results were confirmed by sequencing. BL21DE3 cells transformed with the plasmid were induced for 3 hrs with 1mM IPTG (Sigma) and the bacterial lysate was prepared and incubated with glutathione agarose to pulldown GST-IRS1. The beads were washed twice with lysis buffer and then 2 more times with kinase buffer before use in assays. Phosphorylation reactions were conducted in a 50ul reaction volume in

kinase buffer that contained 25mM Tris (pH7.5), 10mM $MgCl_2$, 2mM DTT, 5mM β-Glycerophosphate, and 0.1mM Na_3VO_4 and 0.2mM ATP. GRK2-stimulated phosphorylation was initiated by the addition of 250ng purified GRK2 (Invitrogen) and 100ng of purified Gβγ complex (Calbiochem) to ensure maximal activation of GRK2. Reactions were carried out for 40min at 30^{o}C and stopped by the addition of 10ul of 6x sample loading dye. Samples were heated for 5 min at 95^{o}C, mixed and centrifuged to pellet the agarose beads. 30ul of each reaction mixture was loaded onto a 4-20% Tris-Glycine gel and after electrophoresis the proteins were transferred to nitrocellulose for western blotting. The phosphorylation of IRS1 was probed using a site-specific antibody to Ser307 (Millipore) and the amount of total IRS1 used in the assay was detected by blotting for GST (SantaCruz). For quantification the amount of phospho-ser307 was normalized to total IRS1 for each reaction.

Echocardiography. To measure global cardiac function, echocardiography was performed 1, 3, 6 and 8 week post-MI in mice and 3, 6 and 12 week post MI in rats by use of the VisualSonics VeVo 770 imaging system with a 710 scanhead in anesthetized animals (2% isoflurane, v/v). The internal diameter of the LV was measured in the short-axis view from M-mode recordings in end diastole and end systole and ejection fraction (EF) and fractional shortening (FS) were calculated using the formulas as previously described[8].

Catheter-based *in vivo* Hemodynamic Measurements. Cardiac function was measured at the appropriate times in mice and rats using a 2 F pressure catheter (SPR-320; Millar instruments, Houston, Texas). The pressure transducer was placed into the LV cavity through the right carotid artery and the right external jugular vein was cannulated with a P-10 catheter (Becton

Dickinson, Sparks, MD) that was used for isoproterenol administration (333 ng/kg BW) as previously described [8].

Plasma membrane isolation, immunoblotting and immunoprecipitation. For plasma membrane isolation, cells were homogenized in buffer containing 25 mM Tris−HCl (pH 7.5), 5 mM EDTA, 5 mM EGTA, 1mM phenylmethylsulfonyl fluoride, 2 μg/ml each leupeptin and aprotinin. In experiments that required detection of phospho-proteins lysis buffers also contained phosphatase inhibitors (Sigma). Intact cells and nuclei were moved by centrifugation at 1,000 × g for 15 min. The collected supernatant was further subject to a centrifugation at 38,000 × g for 1 hour. The pellet was resuspended in lysis buffer (1% Nonidet P−40, 10%glycerol, 137 mM NaCl, 20 mM TrisHCl (pH 7.4), 1 mM phenylmethylsulfonyl fluoride, 20 mM NaF, 1 mM sodium pyrophosphate, 1 mM sodium orthovanadate, and 2 μg/ml each aprotinin and leupeptin) and used as plasma membrane fraction, and the supernatant was used as the cytosolic fraction. Whole cell lysates were prepared in RIPA buffer (50mM Tris−HCl (pH 7,5), 150mM NaCL, 1%NP−40, 0.25% deoxycholate, 9.4mg/50ml sodium orthovanadate, 1% sodium dodecyl sulphate). Protein concentration was determined using BCA assay kit (Pierce). For immunoprecipitation (IP), endogenous IRS1 from whole cell lysates was IP'd with IRS-1 antibody (Cell Signaling) and protein A/G conjugated to agarose beads (Santa Cruz). Samples were rotated overnight at 4°C then centrifuged at 12,000×g for 5 min. IP's were washed twice with lysis buffer, twice with phosphate buffered saline, and suspended in 1× SDS gel loading buffer. Clarified lysates, membrane proteins, or immunocomplexes were resolved by SDS-PAGE on Tris-Glycine gels and transferred to a nitrocellulose membrane. GLUT4 (1:1000, Cell Signaling), Total IRS1 (1:1000 Cell Signaling), GRK2 (1:5000, Santa Cruz), pIRS1 ser307

(1:1000, Millipore), pIRS1 Tyr 612 (1:1000, Sigma), pAkt (1:1000, Cell Signaling), and Total Akt (1:1000, Cell Signaling) were visualized after incubation with fluorescent secondary antibodies using the Odyssey imaging system from LiCor. Quantification of band density was determined using the built-in densitometric software application from LiCor.

Immunofluorescence. ARVMs were plated on glass-bottom dishes (FluoroDish, WPI) pre-coated with laminin (Invitrogen). Following treatment with insulin, standard immunostaining techniques were performed. Briefly, cells were fixed for 15 min using 4% PFA, blocked with 1% BSA/PBS and incubated with primary antibodies against IRS1 (Abcam, ab52167) and GRK2 (Santa Cruz Biotechnology, sc-13143) at 1:50 dilutions. Secondary antibodies conjugated to Alexa Fluor488 and Alexa Fluor568 (Invitrogen), were used at 1:200 dilutions. Images were obtained using Olympus FluoView 500 laser scanning confocal microscope. Control images to examine non-specific staining (background) were obtained using only the secondary antibody.

Group	Time (Weeks)	n	dp/dt max basal (mmHg/s)	dp/dt max Iso (mmHg/s)	dp/dt min basal (mmHg/s)	dp/dt min Iso (mmHg/s)
Sham	3	8	6527±232	15809±573	-8698±302	-10980±257
	6	8	6423±126	15842±248	-8421±214	-10422±203
	12	8	6203±268	15362±185	-8551±252	-10322±233
AAV6GFP	3	8	6246±796	13658±941	-6299±706	-6889±513*
	6	8	6898±168	10669±940*	-5737±506	-6807±520*
	12	8	4736±240	8374±574*	-3203±210	-4563±238*
AAV6βARKct	3	8	6306±803	14131±714	-7171±886	-7581±606*
	6	8	7153±425	13363±845*§	-5867±490	-7250±290*§
	12	8	5045±149	12784±683*§	-5430±150	-7180±120*§

Supplementary Table 1. Hemodynamic measurements in post MI rats. Data are presented as mean ± standard error. Sham: Control group. AAV6GFP: post MI treated with AAV6GFP. AAV6βARKct: post MI treated with AAV6βARKct. dp/dt_{max}: maximum rate of rise of LV pressure ; dp/dt_{min}: maximum rate of fall of LV pressure (* P<0.05 vs Sham; § P< 0.05 vs AAV6GFP). Shown is data at baseline (basal) and after administration of the βAR agonist isoproterenol (Iso 333 ng/Kg – 10 min.). Iso produced significant increase in heart rate over basal condition (data not shown).

Supplementary Figure 1

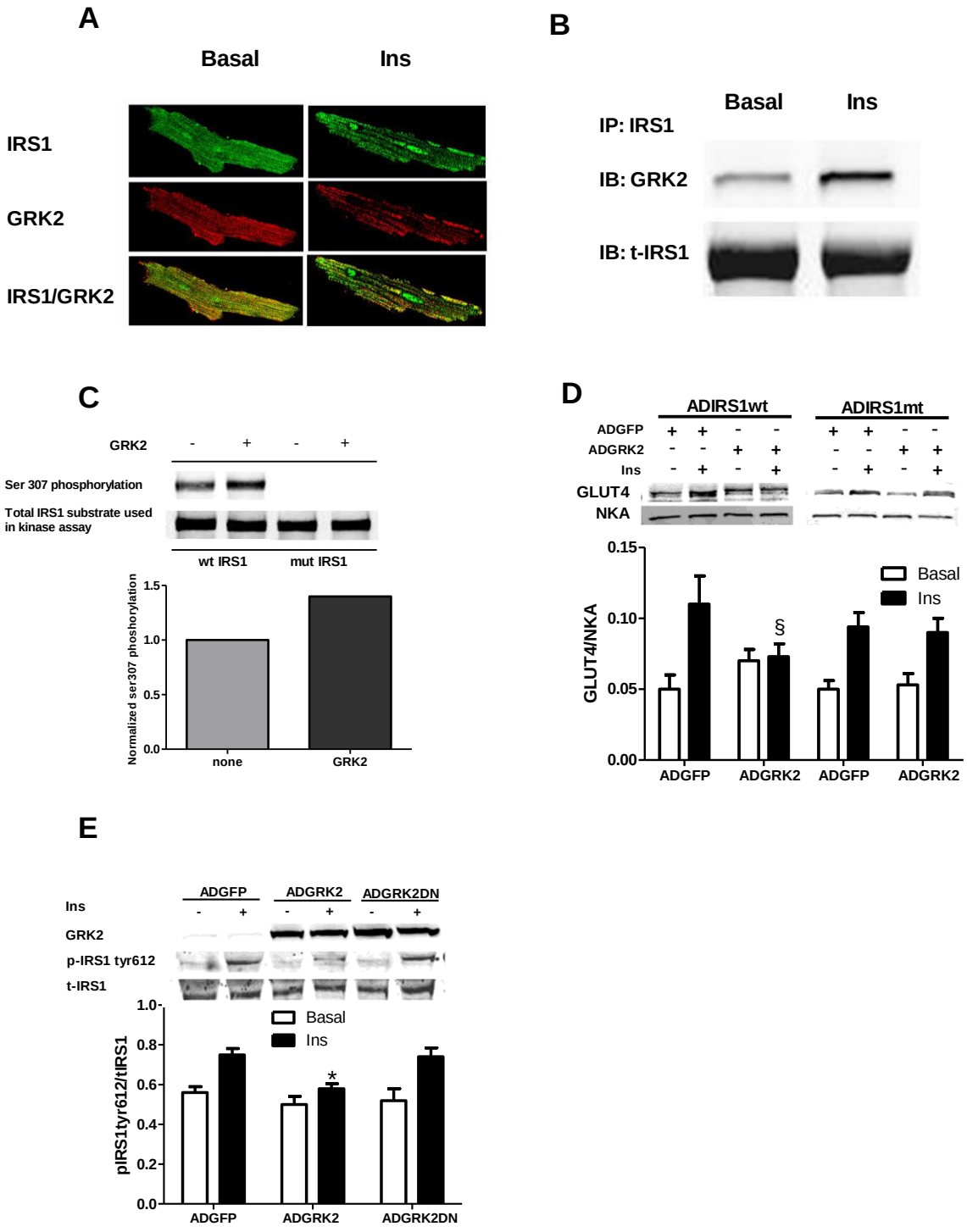

Supplementary Figure 2

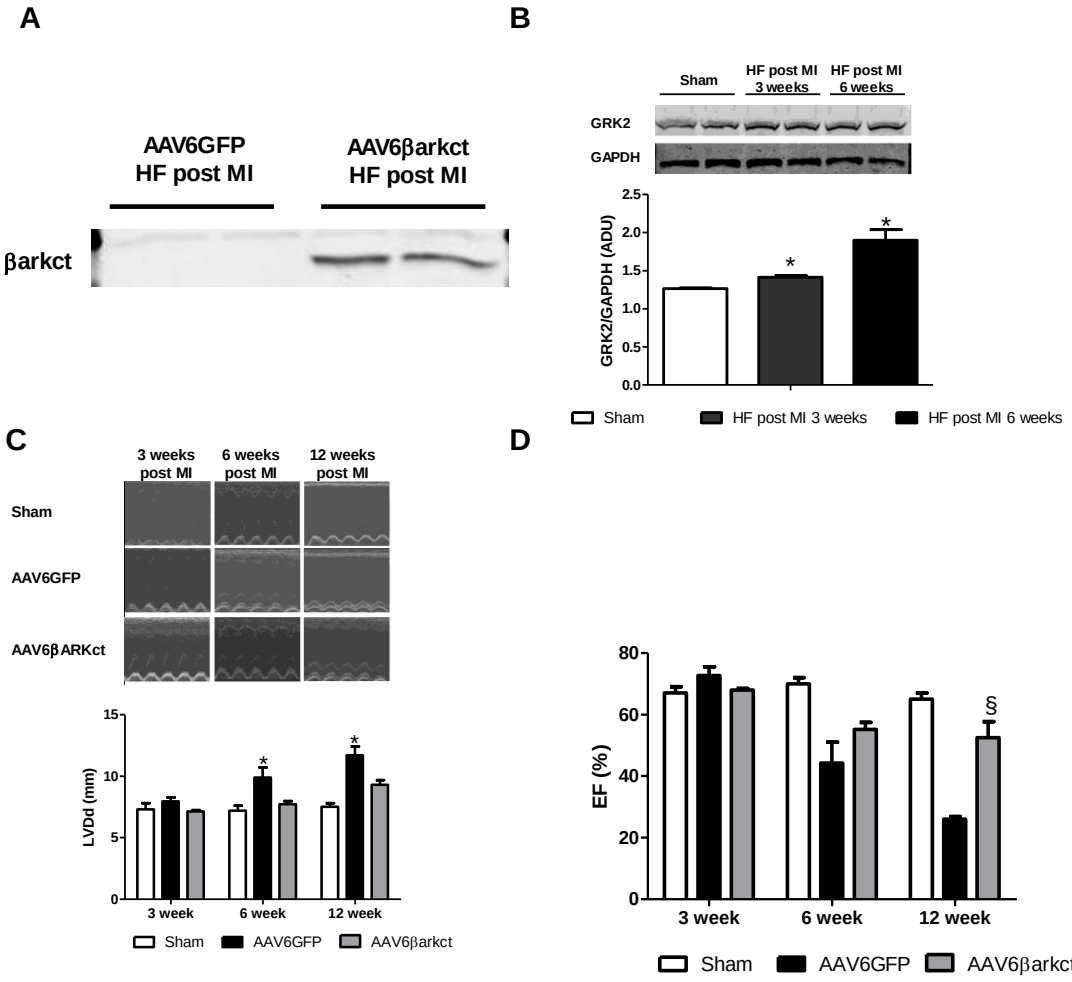

Supplementary figure legends

Supplementary Figure 1. (A) Immunofluorescence assay showing translocation of GRK2 (*red*) and IRS1 (*green*) from cytosol to the plasma membrane in response to Insulin (Ins) treatment (0.1 μM for 10 min). GRK2 and IRS1 co-localization at the plasma membrane is shown in the merged image (*yellow*). This figure is representative of 3 independent experiments. **(B)** GRK2 co-immunoprecipitates with IRS1. IRS1 was immunoprecipitated from whole lysate of ARVMs with or without Ins stimulation. This figure is representative of 3 independent experiments (**C**) GRK2 cannot phosphorylates IRS1mt. Western blot of GRK2-stimulated Ser307 phosphorylation of wild-type or mutant IRS1. Representative blot from 3 independent assays is shown (**D**) ARVMs infected with ADGRK2 (wild-type, WT), ADGFP or a kinase-dead, dominant-negative GRK2 (ADGRK2DN = GRK2-K220R) and stimulated with Ins (0.1 μM for 10 min) were analyzed for Tyr 612 phosphorylation (activating) of IRS1. A representative blot for pTyr 612 IRS1 and total IRS1 and densitometric analysis of three independent experiments is shown in the lower panel (* $P<0.05$, fold of activation, ADGRK2 vs ADGFP and ADGRK2DN, n=3). (**E)** NRVMs were co-infected with either ADIRS1wt or ADIRS1 mutant Ser307Ala (mt) in addition to ADGFP or ADGRK2 and stimulated with Ins as above. Representative blots for GLUT4 and NKA are shown (§, $P<0.01$, fold activation vs ADGRK2+ADIRS1wt, n=3).

Supplementary Figure 2. (A) Representative western blot showing βARKct transgene expression in the heart 3 weeks post surgery and gene delivery compared to a sham operated animal. **(B)** GRK2 up-regulation during HF progression evidenced by western blot in 3 and 6 week post-MI rat hearts compared to sham animals (* $P<0.05$ vs Sham, n=6). (**C**) Cardiac dimensions evaluated by echocardiography in Sham, AAV6GFP, AAV6βARKct treated Rats at

2, 6 and 12 weeks post-MI. Representative M-mode images at the top and histogram showing calculated LV diameter at diastole at the bottom (* $P< 0.01$ vs AAV6βARKct and Sham, n=12). Cardiac function evaluated by Echocardiography as Ejection Fraction (§ $P< 0.01$ vs Sham and AAV6βARKct, n=12).

Supplementary References

1. O'Connell TD, Rodrigo MC, Simpson PC. Isolation and culture of adult mouse cardiac myocytes. *Met Mol Biol* 2007;357:271-296.

2. DeGeorge BR, Jr., Gao E, Boucher M, Vinge LE, Martini JS, Raake PW, Chuprun JK, Harris DM, Kim GW, Soltys S, Eckhart AD, Koch WJ. Targeted inhibition of cardiomyocyte Gi signaling enhances susceptibility to apoptotic cell death in response to ischemic stress. *Circulation.* Mar 18 2008;117(11):1378-1387.

3. Gao E, Lei YH, Shang X, Huang ZM, Zuo L, Boucher M, Fan Q, Chuprun JK, Ma XL, Koch WJ. A Novel and Efficient Model of Coronary Artery Ligation and Myocardial Infarction in the Mouse. *Circ Res.* 2010; 107:1445-1453.

4. Raake PW, Vinge LE, Gao E, Boucher M, Rengo G, Chen X, DeGeorge BR, Jr., Matkovich S, Houser SR, Most P, Eckhart AD, Dorn GW, 2nd, Koch WJ. G protein-coupled receptor kinase 2 ablation in cardiac myocytes before or after myocardial infarction prevents heart failure. *Circ Res.* 2008;103:413-422.

5. Rengo G, Lymperopoulos A, Zincarelli C, Donniacuo M, Soltys S, Rabinowitz JE, Koch WJ. Myocardial adeno-associated virus serotype 6-betaARKct gene therapy improves cardiac function and normalizes the neurohormonal axis in chronic heart failure. *Circulation.* 2009;119:89-98.

6. Fang YH, Muzic RF, Jr. Spillover and partial-volume correction for image-derived input functions for small-animal 18F-FDG PET studies. *J Nucl Med.* 2008;49:606-614.

7. Cheng L, Ding G, Qin Q, Huang Y, Lewis W, He N, Evans RM, Schneider MD, Brako FA, Xiao Y, Chen YE, Yang Q. Cardiomyocyte-restricted peroxisome proliferator-

activated receptor-delta deletion perturbs myocardial fatty acid oxidation and leads to cardiomyopathy. *Nat Med.* 2004;10:1245-1250.

8. Lymperopoulos A, Rengo G, Funakoshi H, Eckhart AD, Koch WJ. Adrenal GRK2 upregulation mediates sympathetic overdrive in heart failure. *Nat Med.* 2007;13:315-323.

G Protein–Coupled Receptor Kinase 2(GRK2)의 억제를 통한 심근기능의 향상이 가능하다 : 인슐린저항성을 높이는 GRK2의 새로운 면모

한 기 훈 교수 서울아산병원 심장내과

Summary

배경

신경 또는 체액에 기반한 자극신호로 조절되는 심장의 에너지대사는 심부전의 병태생리에 중요한 역할을 수행한다. 만성적인 adrenergic stimulation은 심부전을 유발/악화시키지만, 한편으로는 G protein–coupled receptor kinase 2(GRK2)의 활성을 높이는바, 이는 beta adrenergic receptor(BAR) 시스템의 와해와 유관한 심근세포의 병적인 진행을 일으키는 현상이다. 본 연구에서는 GRK2의 발현 및 활성이 증대되는 심부전에서 관찰되는 현상이 심장의 대사에 악영향을 미치는가를 규명하였다.

방법 및 결과

Positron emission tomography(PET) 연구에서 심장에 특이적으로 GRK2 과발현을 이룬 transgenic mice들은 당의 함입을 저해하고 insulin 전달신호를 desensitization 시킴으로써 심근대사를 저해함을 나타냈으며, 이는 허혈성 손상 이후에 발생하며 심부전 이전에 출현함을 증명하였다. 기전적으로 GRK2는 cardiomyocytes의 insulin receptor substrate-1을 직접적으로 상호작용하여 인산화시키고, GLUT4 등이 membrane translocation되는 것을 저해하는 등의 인슐린 의존성 negative signaling feedback을 유도한다. 이는 insulin receptor substrate-1이 비수용체성 GRK2의 목표임을 의미하며, GRK2가 기능이 저하되는 심장의 치료적인 목표가 될 수 있음을 보여준다. 즉, GRK2 활성도를 억제할 때 허혈성 상태 이후의 장애를 심근의 인슐린 신호전달을 변화시켜 심근세포의 당함입을 유지하게 되므로 GRK2를 타겟으로 한 심부전의 치료가 가능할 것이다.

결론

본 연구결과는 GRK2가 손상을 받은 심장에서 어떻게 병적인 기능을 하는지에 대하여 보여준다. GRK2의 역할은 심근의 수축력을 결정하는 인슐린 신호 및 BAR의 신호체계가 기전적으로 상호연계되어 있음을 나타낸다.

GRK2란?

GRK2[G protein coupled receptor(GPCR) kinase 2]는 GPCR의 인산화를 통하여 beta-arrestin을 결합시켜 수용체의 internalization 및 desensitization을 유발하는 classic한 작용 이외에도 다양한 물질들의 인산화를 유발하여 세포기능을 조절하며 GPCR의 alpha, beta-gamma unit에도 작용하여 세포신호를 제어한다.

GRK는 잘 보존된 central catalytic domain(~270aa), serine-threonine kinase와 유사한 구조, 수용체를 주로 인지하는 N-terminal domain(~185aa)과 다양한 길이 및 서열을 보이는 carboxyl-terminal domain(~105–230aa)들로 구성되어 다양한 기능을 보일 수 있다. N-terminal domain에는 120aa정도의 길이를 가지는 RH domain(regulator of G protein signalling homology domain)이 존재하여 Gaq와의 결합을 통하여 phospholipase C beta(PLCβ)가 활성화하는 것을 저해하고, C-terminal domain에는 pleckstrin homology domain(PH)이 존재하여 PIP2와 free Gβγ subunits과의 상호작용을 통하여 이들이 세포막으로 이동하는 것을 유도하기도 한다.

GRK는 GPCR뿐 아니라, IGF-1, insulin, PDGF, EGF 등을 매개하는 tyrosine kinase 수용체의 활성에도 관여한다. 특히, GRK2는 tubulin, synucleins, phosducin, ribosomal protein P2, the inhibitory γ subunit of the type 6 retinal cyclic guanosine monophosphate(cGMP) phosphodiesterase, a subunit of the epithelial Na^+ channel, the ERM family protein ezrin, the calcium-binding protein DREAM, IKappaBalpha, p38 MAPK 등의 세포막에 존재하지 않는 다양한 신호전달 물질과도 상호작용한다. 이러한 GRK2의 작용은 현재에도 계속 발견되고 있을 뿐 아니라, α-actinin, clathrin, calmodulin, caveolin, RKIP 등과의 상호작용을 통하여 GRK2의 발현도, 세포내 분포 등을 조절하기도 한다. 특히, GRK2는 3, 5, 6형과 더불어 조직에 광범위하게 분포하기 때문에 세포 유형에 따른 반응의 특징을 보이기도 한다.

염증세포 등의 경우 특정 chemokine 수용체의 desensiti-zation에 관여하며, 주로 이동하는 선행부에 분포하므로 GRK2의 활성이 저하되면 세포 이동이 활발해 진다. 한편으로, epithelial cell이나 fibroblast 등에서는 수용체의 활

Figure 1. 대표적인 GRK2형의 세포내 신호전달 조절 효과

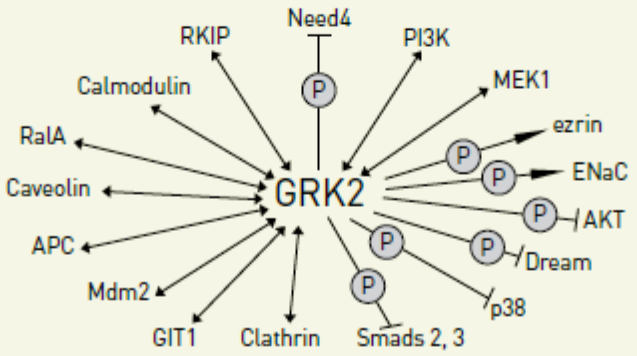

성을 높여 fibronectin 등에 매개한 세포의 adhesion이나 이동을 촉진시키기도 한다.

심근세포에서는 beta-adrenergic signalling에 관여하는데 GRK2 활성을 저해시키면 카테콜아민에 의한 반응이 증대되어 수축력이 향상되고 기능이 좋아진다. GRK2의 활성도가 심근의 기능이 저하된 심부전 상태에서 높게 측정된다는 보고는 매우 흥미로우며, 실험적으로는 GRK2의 활성을 증가시킬 때 심부전 상태가 유도된다고 하므로 이 활성도를 조절하는 것이 심부전의 치료목적으로 유용할 것이라는 가능성이 높게 존재한다. 특히, 심근경색 후에 GRK2 활성도를 억제하면 이후에 유발될 수 있는 심부전 상태를 예방할 수 있을 것이다.

심근세포에서 GRK2의 새로운 기능: 인슐린저항성을 증가시킴

본 연구는 이러한 GRK2의 심근세포에 대한 기능을 이해하는 연장선상으로서 GRK2의 활성도가(심근경색으로 인하여) 증대된다면, GLUT4의 활성이 둔화되고 따라서 심근 기능이 저해됨을 보여준다. 이러한 배후기전으로 GRK2에 의한 insulin receptor substrate-1(IRS-1) 수용체의 직접적인 인산화가 기여할 것이라는 점을 증명하였다. 특히, Ser307의 인산화가 중요하며, 이는 IRS1 phospho-Tyr binding domain 바로 직전에 위치하며 GRK2에 의한 인산화는 본 수용체의 desensitization을 유발하여 인슐린저항성을 상승시킨다는 측면에서 beta-adrenergic receptor의 desensitization 기전과 유사한 측면을 보인다고 할 수 있다. 이러한 기전에 의한 인슐린저항성은 비단 심근세포에만 관찰되는 것은 아니며, 지방세포 등에서도 관찰되는 것으로 보인다. 심근경색 이후의 심근 기능의 제고를 위한 단기치료가 가능하다는 점, GRK2의 광범위한 분포가 위험요소이기는 하지만 인슐린저항성의 개선이라는 측면에서 긍정적이라는 점을 고려하면 GRK2의 억제로 얻을 수 있는 이득이 극대화되는 임상적 상황이 존재하고 이러한 시점에서의 치료적인 효용이 기대된다고 할 수 있겠다.

References

1. Pemela P, Murga C, Ribas C, Lafarga V, Mayor F Jr. The complex G protein-coupled receptor kinase 2 (GRK2) interactome unveils new physiopathological targets. *Br J Pharmacol* 2010;160: 821–832.